Cell

EXTENDED EXPERIMENTAL PROCEDURES

Protein Purification

A list of expression plasmids generated in this study is provided (Table S4). The gene encoding *K. polysporus* Dcr1ΔC was cloned into a modified pRSFDuet vector (Novagen) containing an amino-terminal Ulp1-cleavable His_6-Sumo tag. Protein was overexpressed in *E. coli* BL21(DE3) Rosetta2 (Novagen). Cells expressing the recombinant protein were lysed by sonication in Buffer A (10 mM phosphate buffer pH 7.3, 640 mM NaCl, 25 mM imidazole, 10 mM β-mercaptoethanol (β-ME), 1 mM phenylmethylsulphonyl fluoride), and the lysates were cleared by centrifugation. The supernatant was loaded onto a nickel column and then washed with Buffer A. The target protein was eluted with a linear gradient of 25 mM to 1 M imidazole. The protein fractions were collected and dialyzed against Buffer B (10 mM phosphate buffer pH 7.3, 500 mM NaCl, 20 mM imidazole, 10 mM β-ME) overnight. Ulp1 protease was added, and the digested protein was loaded onto a nickel column to remove the cleaved His_6-Sumo tag. Ammonium sulfate was added to the flow-through containing Dcr1ΔC, and the sample was centrifuged. The supernatant was loaded onto a phenyl-sepharose hydrophobic interaction column in Buffer C (10 mM phosphate buffer pH 7.3, 2 M ammonium sulfate, 10 mM β-ME), and the protein was eluted with a linear gradient of 1 to 0 M ammonium sulfate. The eluted protein was dialyzed against Buffer D (100 mM Na/K-phosphate buffer pH 7.3, 10 mM β-ME) and then loaded onto a Heparin-affinity column in Buffer B. The protein was eluted with a linear gradient of 0 to 2 M NaCl. The eluted sample was dialyzed against Buffer D and then loaded onto a MonoQ column in Buffer D. The protein was eluted with a linear gradient of 0 to 2 M NaCl. The eluted sample was concentrated and loaded onto a HiLoad 200 16/60 column in Buffer E (10 mM Tris-HCl pH 7.5, 200 mM NaCl, 5 mM DTT). The final two purification steps (MonoQ and HiLoad 200 columns) were performed 1–3 times, until contaminating nucleic acids were no longer present as judged by UV absorbance (A_{280}/A_{260}). Purified Dcr1ΔC was concentrated to approximately 20 mg ml^{-1} using ultrafiltration and stored at −80°C in Protein Storage Buffer (10 mM Tris-HCl pH 7.5, 200 mM NaCl, 5 mM DTT).

Point substitutions were introduced using site-directed mutagenesis. Full-length Dcr1, selenomethionine (SeMet)-substituted Dcr1ΔC, active-site Dcr1ΔC mutants, Dcr1ΔNΔC, and Dcr1ΔC variants containing *Gi*Dicer VL-1 or VL-2 with or without the E224Q mutation were purified essentially as described above for wild-type Dcr1ΔC, except full-length Dcr1 contained contaminating nucleic acids and was stored in a different buffer (10 mM Tris-HCl pH 8.5, 600 mM NaCl, 10 mM β-ME). Both of the Dcr1ΔC VL-1 and VL-2 variants eluted from the gel filtration column at the same retention time as wild-type Dcr1ΔC, suggesting that they are correctly folded (data not shown). Dcr1Δ2d and E224Q Dcr1Δ2d were overexpressed as His_6-Sumo tag fusion proteins as described for Dcr1ΔC. After removal of the cleaved His_6-Sumo tag, the proteins were loaded onto a Heparin-affinity column in Buffer D. The protein was eluted with a linear gradient of 0 to 2 M NaCl. Ammonium sulfate was added to the eluted fractions, and the sample was centrifuged. The supernatants were loaded onto a phenyl-sepharose hydrophobic interaction column in Buffer C, and the protein was eluted with a linear gradient of 1 to 0 M ammonium sulfate. The eluted samples were concentrated and loaded onto a HiLoad 200 16/60 column in Buffer E.

Structure Determination and Refinement

Native crystals of Dcr1ΔC were obtained at 20°C by sitting-drop vapor diffusion in 0.18 M triammonium citrate, 20% PEG3350, 10 mM Na-HEPES buffer (pH 7.5), 20 mM magnesium chloride, and 3% 2-propanol. SeMet-substituted crystals were grown at 20°C by sitting-drop vapor diffusion in 220 mM Na-malonate buffer (pH 7.0), 15% PEG4000, and 10 mM phenol. The native and SeMet-substituted crystals of Dcr1ΔC were soaked in collection buffer (1.2-fold concentrated reservoir solution), cryoprotected with 10% glycerol, and flash-cooled in a nitrogen stream at 100 K. Both derivative data sets were collected at Brookhaven NSLS beamline X29. Data were processed with the program HKL2000 (Otwinowski and Minor, 1997). Data collection and refinement statistics are shown in Table S2. A total of 20 selenium sites were found using peak data with the program SnB (Weeks and Miller, 1999) and were used for phase calculation at 3.5 Å resolution with the program SHARP (de La Fortelle and Bricogne, 1997). The initial phases were improved by solvent flattening with the program SOLOMON (Abrahams and Leslie, 1996) and by non-crystallographic symmetry averaging with the program CCP4 (Collaborative Computational Project, 1994). The initial model was built manually with the programs O (Jones et al., 1991) and Coot (Emsley and Cowtan, 2004) and was improved by iterative cycles of refinement with the program Phenix (Adams et al., 2002), which provided a clear electron density map for the N-terminal and RNase III domains. Molecular replacement was performed with the program MOLREP (Vagin and Teplyakov, 2000), using the SeMet structure as a search model. Further model building and refinement revealed electron peaks in the *Fo*–*Fc* density map for one of the four dsRBD1s in the asymmetric unit. The model using the native data was improved to 2.3 Å resolution for the four Dcr1ΔC molecules in the asymmetric unit. Two of the four molecules had completely disordered dsRBD1s, one had a poorly defined dsRBD1, and the other had a well-defined dsRBD1; only the latter was included in the final coordinates. The Ramachandran plot analysis by PROCHECK (Collaborative Computational Project, 1994) showed 93.1% and 6.9% of the protein residues in the most favorable and additionally allowed regions, respectively, with no residues in disallowed regions. The *Fo*−*Fc* simulated annealing omit map was calculated by CNS (Brunger et al., 1998), and the resultant map showed clear octahedral coordination around active-site residues.

Native crystals of E224Q Dcr1Δ2d were obtained at 20°C by sitting-drop vapor diffusion in 0.2 M L-proline, 0.1 M HEPES pH 7.5, and 10% PEG3350. The crystals were soaked in collection buffer (1.2-fold concentrated reservoir solution), cryoprotected with 30% glycerol, and flash-cooled in a nitrogen stream at 100 K. The derivative data set was collected at Advanced Photon Source NE-CAT

beamlines. Molecular replacement performed with MOLREP (Vagin and Teplyakov, 2000) using the structure of the NTD and RNase III domains from Dcr1ΔC as a search model revealed the entire molecule. Model building and refinement were done using Coot (Emsley and Cowtan, 2004) and PHENIX (Adams et al., 2002), respectively. The electron density for the swapped segment within the RNase III domain dimer could be clearly traced in the simulated annealing omit map (*Fo*−*Fc*) with CNS (Brunger et al., 1998).

dsRNA Modeling

In Figure 4E, two molecules of the *Aa*RNase III–dsRNA complex (PDB code 2NUF) and a 47 bp dsRNA (PDB code 3CIY) (Liu et al., 2008) were structurally aligned based on their bound dsRNA such that the RNA cleavage sites were 23 nt apart on the dsRNA. Then, two Dcr1ΔC dimers were structurally aligned onto the homodimeric RNase III domains of the docked *Aa*RNase III molecules.

Preparation of RNA Substrates

dsRNA substrates were prepared by annealing of ssRNA generated by in vitro transcription with T7 RNA polymerase. PCR-generated templates were used for transcription of > 76 nt RNAs, and gel-purified DNA oligonucleotides were used for transcription of shorter RNAs. Transcription reactions for substrates used in single-turnover processing reactions were assembled using the MAXIscript Kit (Ambion) with a 61:1 molar ratio of UTP:[α-^{32}P]UTP (800 Ci/mmol) according to the manufacturer's directions. High specific-activity substrates for use in binding reactions were transcribed with a 2:1 (70–280 nt RNAs) or 16:1 (20–30 nt RNAs) molar ratio of UTP:[α-^{32}P]UTP (800 Ci/mmol). Trace-labeled RNA used for analysis of multiple-turnover kinetics was transcribed with a 3125:1 molar ratio of UTP:[α-^{32}P]UTP. DNase-treated ssRNA was fractionated by denaturing PAGE, eluted from gel slices in 0.3 M NaCl overnight at 4°C, and ethanol precipitated. Complementary RNAs were combined in dsRNA Annealing Buffer (30 mM Tris-HCl pH 7.5, 100 mM NaCl, 1 mM EDTA), heated to 90°C for 1 min, and slowly cooled to room temperature over 4–5 hr. Annealed RNA was fractionated by native PAGE (with the exception of 500 bp dsRNA, which was fractionated on a 4% urea gel), and dsRNA was eluted from gel slices in 0.3 M NaCl overnight at 4°C, ethanol precipitated, and stored in dsRNA Storage Buffer (10 mM Tris-HCl pH 7.5, 10 mM NaCl, 0.1 mM EDTA). RNA was quantified by scintillation counting, and 10X stocks were prepared in dsRNA Storage Buffer supplemented with 1 μM yeast tRNA (Sigma). Body-labeled dsRNA substrates containing 5′-monophosphate termini were prepared similarly, except that gel-purified ssRNA was treated with calf intestinal phosphatase, phosphorylated with T4 polynucleotide kinase, and gel-purified by denaturing PAGE. End-labeled dsRNA substrates were prepared similarly, except radiolabeled UTP was omitted from transcription reactions and phosphorylation was performed with a 32:1 molar ratio of ATP:[γ-^{32}P]ATP (6000 Ci/mmol) before chasing with 1 mM ATP. Substrates used in glutaraldehyde crosslinking experiments were prepared as described in the section on glutaraldehyde crosslinking.

The substrates used in Figure 5D were initially prepared as a single body-labeled dsRNA substrate (1724:1 molar ratio of UTP:[α-^{32}P]UTP) containing 5′-monophosphate termini as described above. This dsRNA was treated with T4 RNA Ligase 1 (NEB) and products were resolved by denaturing PAGE (8% acrylamide, 90% formamide). The incomplete ligation reaction gave rise to unligated duplex (substrate A), hairpin RNA (substrate B), and closed dsRNA (substrate C), which were distinguished by comparison with control ligation reactions using dsRNA containing 5′-triphosphate termini at one or both ends (Figure S5A). Gel-purified RNA was quantified by scintillation counting, and 300 nM stocks were prepared in dsRNA Storage Buffer. The covalently closed nature of substrate C was subsequently confirmed by limited hydrolysis under alkaline conditions, which nicks the RNA to generate slower-migrating species with mobilities that are comparable to the mobility of the hairpin RNA (Figure S5B).

The substrates used in Figure 5E were designed to contain 161 bp of duplex RNA of equivalent specific activity. Substrate D was prepared as a body-labeled dsRNA (3781:1 molar ratio of UTP:[α-^{32}P]UTP) containing 5′-monophosphate termini as described above. The DNA template used for transcription of substrate E was prepared by PCR amplification of supercontig712:108196–108786(–) from *S. castellii* genomic DNA, with the addition of an upstream T7 promoter. The palindromic RNA substrate was transcribed with a 3946:1 molar ratio of UTP:[α-^{32}P]UTP; DNase-treated RNA was fractionated by denaturing PAGE (8% acrylamide, 90% formamide); and the full-length product was eluted from gel slices in 0.3 M NaCl. Substrate F consisted of a body-labeled capped and polyadenylated (A_{20}) ssRNA annealed to an unlabeled ssRNA. The body-labeled RNA was prepared by transcription with a 1579:1 molar ratio of UTP:[α-^{32}P]UTP from a PCR template coding for 20 terminal A residues. Gel-purified ssRNA was enzymatically capped using the ScriptCap m^{7}G Capping System (Epicenter Biotechnologies) and purified by denaturing PAGE. Unlabeled ssRNA was transcribed without radiolabeled UTP and purified by denaturing PAGE. The labeled strand was combined with a 10% excess of the unlabeled strand in dsRNA Annealing Buffer, dsRNA was annealed by heating to 90°C for 1 min and slowly cooling to room temperature, and RNA was concentrated by ethanol precipitation. All RNAs were resuspended in dsRNA Storage Buffer and quantified by scintillation counting, and 300 nM stocks were prepared in dsRNA Storage Buffer.

Dicer Activity Assays

Yeast Extracts

Preparation of whole-cell extracts and processing reactions were performed as described in Drinnenberg et al. (2009) with the following modifications. Substrates were used at a final concentration of ~45 pg/μl (corresponding to ~140 pM for 500 bp dsRNA and ~280 pM for 500 nt ssRNA). Reactions were incubated at room temperature (22–24°C) for 15 min (*K. polysporus*) or 2 hr (*S. castellii*) and stopped by addition of phenol-chloroform and EDTA.

K. polyporus Dcr1

For biochemical assays, proteins were diluted and stored at –20°C in Protein Dilution Buffer (5 mM Tris-HCl pH 7.5, 100 mM NaCl, 2.5 mM DTT, 50% glycerol, 1 mg/ml Ultrapure BSA [Ambion]). All Dcr1 protein concentrations are expressed in terms of dimer concentration. 10 μl reactions contained 2 μl 5X reaction buffer (150 mM Tris-HCl pH 7.5, 150 mM NaCl, 25 mM $MgCl_2$, 5 mM DTT, 0.5 mM EDTA), 1 μl Dcr1 protein or Protein Dilution Buffer, and 1 μl RNA substrate. All reactions were under standard single-turnover conditions, unless otherwise indicated. Standard single-turnover reactions contained protein at a final concentration of 30 nM and RNA at a final concentration of ~45 pg/μl (corresponding to ~1 nM for 70 bp dsRNA). Reactions were incubated at room temperature (22–24°C) for 90 s unless otherwise indicated and quenched by addition to 10 μl Formamide Loading Buffer (90% formamide, 18 mM EDTA, 0.025% sodium dodecyl sulfate, 0.1% xylene cyanol, 0.1% bromophenol blue). Multiple-turnover reactions in Figures 6A and 6B contained protein at a final concentration of 10–30 nM as indicated and 70 bp dsRNA at a final concentration of ~4.5 ng/μl (corresponding to ~100 nM); multiple-turnover reactions in Figure S6E were supplemented with NaCl to obtain the indicated final concentration, and contained protein at a final concentration of 30 nM and 500 bp dsRNA at a final concentration of ~4.5 ng/μl (corresponding to ~14 nM). Reactions were incubated at room temperature, and 4 μl aliquots were removed at the indicated time and quenched by addition to 12 μl Formamide Loading Buffer. Multiple-turnover reactions in Figures 5D and 5E and Figure S5C contained protein at a final concentration of 10 nM and substrates at a final concentration of ~30 nM. 5 μl reactions were incubated at room temperature for 90 s and quenched by addition of 15 μl Formamide Loading Buffer.

Human Dicer

Recombinant *H. sapiens* Dicer (0.5 U/μl, Genlantis) was combined with an equal volume of Protein Dilution Buffer. 10 μl reactions contained 2 μl 5X reaction buffer (150 mM Tris-HCl pH 6.8, 125 mM NaCl, 15 mM $MgCl_2$, 5 mM DTT, 0.5 mM EDTA, 5% glycerol), 1 μl Dicer (0.25 U/μl), and 1 μl RNA substrate. Reactions were incubated at 37°C for 15 min (Figure 5B) or 30 min (Figure 4D) and quenched by addition to 10 μl Formamide Loading Buffer.

Drosophila Dcr-2

Purified recombinant *D. melanogaster* Dcr-2 (expressed using the baculovirus system) was a generous gift from Phil Zamore (University of Massachusetts Medical Center). 5 μl reactions contained 1 μl 5X reaction buffer (150 mM Tris-HCl pH 6.8, 125 mM NaCl, 15 mM $MgCl_2$, 5 mM DTT, 0.5 mM EDTA, 5% glycerol), 0.5 μl 10 mM ATP, 0.5 μl *Dm*Dcr-2 protein or Dcr-2 Storage Buffer (60 mM HEPES-KOH pH 7.4, 400 mM NaCl, 4 mM DTT, 50% glycerol), and 0.5 μl RNA substrate. *Dm*Dcr-2 was present at a final concentration of ~10.6 nM, and RNA was at a final concentration of ~30 nM for each substrate. Reactions were incubated at room temperature for 30 min (Figure 5D and Figure S5C) or 5 min (Figure 5E) and quenched by addition of 15 μl Formamide Loading Buffer.

Analysis

RNA products were resolved by 7.5 M urea 15% PAGE, unless otherwise indicated. Radiolabeled products were visualized by phosphorimaging (Fujifilm BAS-2500) and quantified using Multi Gauge (Fujifilm). To quantify product formation in Figures 5D and 5E and Figure S5C, the percent product was measured as P_P = 100*[siRNA product]/([siRNA product] + [substrate]), and the background P_P value (calculated from the corresponding –Dicer control lane) was subtracted. For quantitative analysis of multiple-turnover kinetics in Figure 6B, at each time point (t) the fraction product was measured as F_P = [23 nt product]/([23 nt product] + [70 nt substrate]). Data were fit to the burst equation:

$$F_P = A\left(1 - e^{-kt}\right) + bt,$$

where A was the burst amplitude, k was the exponential burst rate constant, and b was the linear steady-state velocity. Fits were performed using the nonlinear least-squares method implemented in KaleidaGraph (Synergy Software).

Dicer Binding Assays

10 μl reactions contained 2 μl 5X binding buffer (150 mM Tris-HCl pH 7.5, 150 mM NaCl, 25 mM $MgCl_2$, 5 mM DTT, 0.5 mM EDTA, 25% glycerol), 1 μl protein, and 1 μl RNA substrate, with the exception of reactions in Figure S6D which were supplemented with an additional 109 mM NaCl. E224Q Dcr1ΔC was present at the indicated final concentration, and RNA was present at a final concentration of ~450 fg/μl (corresponding to ~10 pM for 70 bp dsRNA) for 70–280 bp substrates or ~11.6 pg/ul (corresponding to ~400 pM for 30 bp dsRNA) for 20–30 bp substrates. Reactions were incubated at room temperature (22–24°C) for 10 min and then on ice for at least an additional 20 min. Reactions were analyzed on native polyacrylamide gels (6% 29:1 acrylamide:bis-acrylamide, 0.5X TBE, 5 mM $MgCl_2$, 5% glycerol) cooled to 4°C. Samples were loaded without addition of loading buffer, and gels were run at 10W for 2.5 hr at 4°C in 0.5X TBE supplemented with 5 mM $MgCl_2$. RNA was visualized by phosphorimaging (Fujifilm BAS-2500) and quantified using Multi Gauge (Fujifilm). At each concentration (P), the fraction bound (as designated in Figure S6B) was measured as F_B = $dsRNA_{bound}$/($dsRNA_{bound}$ + $dsRNA_{free}$). Data were fit to the Hill equation:

$$F_B = A + B/\left[1 + (K_D/P)^n\right],$$

where *A* was background signal, *B* was the magnitude of the dynamic range, K_D was the apparent dissociation constant, and *n* was the Hill coefficient. To fit binding data for the 20 bp dsRNA substrate, *B* was set equal to 1.0. Fits were performed using the nonlinear least-squares method implemented in KaleidaGraph (Synergy Software).

Multi-Angle Light Scattering

Molecular-weight experiments were undertaken on a three-angle light scattering detector (mini-DAWN EOS) and refractive index detector (Optilab DSP, Wyatt Technology). Data were collected every 0.5 s at a flow rate of 0.2 ml per min. Data analysis was carried out using the program ASTRA, yielding the molar mass and mass distribution of the sample. The middle portion of the peak saturated the refractive-index detector, and hence the analysis was restricted to the shoulders of the peak (Figure S2B). The red and green lines represent molecular mass as a function of elution volume.

Glutaraldehyde Crosslinking

Radiolabeled Nucleic Acids

dsRNA substrates were prepared by annealing of body-labeled ssRNA containing 5′-monophosphate termini, which were generated as described above except that 1257:1 and 1571:1 molar ratios of UTP:[α-^{32}P]UTP were used for transcription of 70 nt and 500 nt ssRNAs, respectively. 70 bp dsDNA was prepared by annealing of end-labeled ssDNA, which was generated by phosphorylating gel-purified DNA oligonucleotides using a 571:1 molar ratio of ATP:[γ-^{32}P]ATP (6000 Ci/mmol) before chasing with 1 mM ATP. End-labeled 500 bp dsDNA was prepared by phosphorylating PCR primers using a 77:1 molar ratio of ATP:[γ-^{32}P]ATP (6000 Ci/mmol) before chasing with 1 mM ATP, and then performing PCR using the end-labeled primers. Gel-purified dsRNA and dsDNA were eluted from gel slices in 0.3 M NaCl overnight at room temperature, ethanol precipitated, and stored in Crosslinking Storage Buffer (10 mM HEPES-NaOH pH 7.6, 10 mM NaCl, 0.1 mM EDTA). dsDNA and dsRNA were quantified by absorbance at 260 nm, and 10X stocks (986 nM for 70 bp substrates and 138 nM for 500 bp substrates, each corresponding to 3 μM non-overlapping 23 bp fragments) were prepared in Crosslinking Storage Buffer.

Protein-Only Reactions

Dcr1ΔC and Dcr1ΔNΔC were prepared as 10 μM stocks in BSA-Free Protein Dilution Buffer (5 mM Tris-HCl pH 7.5, 100 mM NaCl, 2.5 mM DTT, 50% glycerol), stored at –20°C, and centrifuged at 4°C for 10 min at 16100*g* to remove any aggregates before using. 10 μl crosslinking reactions contained 2 μl 5X Crosslinking Reaction Buffer (150 mM HEPES-NaOH pH 7.6, 150 mM NaCl, 25 mM $MgCl_2$, 5 mM DTT, 0.5 mM EDTA), 0.3 μl 10 μM protein, and 2 μl freshly diluted glutaraldehyde (5X indicated final concentration, Sigma). Reactions were incubated at room temperature for 10 min, quenched by addition of 10 μl Crosslinking Quench Buffer (2X Laemmli Sample Buffer, supplemented with 5% β-ME and 100 mM Tris-HCl pH 8.0), and incubated for an additional 10 min. Quenched reactions were separated by SDS-PAGE (4%–12% NuPAGE Novex Bis-Tris Mini Gels in MOPS SDS Running Buffer, Invitrogen) and analyzed by silver staining.

Reactions with RNA/DNA

E224Q Dcr1ΔC was prepared for crosslinking as described above. 44 μl binding reactions contained 11 μl 5X Crosslinking Reaction Buffer, 1.65 μl 10 μM E224Q Dcr1ΔC, and 5.5 μl Crosslinking Storage Buffer or 10X RNA/DNA. Binding reactions were incubated at room temperature for 10–20 min before initiating the crosslinking reactions. 8 μl aliquots of the binding reactions were mixed with 2 μl glutaraldehyde, incubated at room temperature for 10 min, quenched by addition of 10 μl Crosslinking Quench Buffer, and incubated for an additional 10 min. Quenched reactions were separated by SDS-PAGE and analyzed by silver staining. Radiolabeled nucleic acids were visualized by phosphorimaging of the silver-stained gel. To confirm the formation of Dicer-dsRNA complexes, 8 μl aliquots of the binding reactions (including negative control reactions with BSA substituted for E224Q Dcr1ΔC) were mixed with 2 μl 25% glycerol, incubated on ice for 10–20 min, and analyzed on native polyacrylamide gels as described for the dicer binding assays.

Yeast Manipulations

Growth Conditions and Genetic Manipulations

S. castellii and *K. polysporus* were grown at 25°C (with the exception of strains in Figure S5D, which were grown at 30°C) on standard *S. cerevisiae* plate and liquid media (e.g., YPD and SC). Transformations of *S. castellii* were performed as described in Drinnenberg et al. (2009) with some modifications. Either 1.5 μg plasmid DNA or 10 μg linear DNA was added to 5 μl single-stranded DNA (10 mg/ml salmon sperm DNA, Sigma D7656), mixed with 50 μl yeast (~3 × 10^8 cells in 100 mM lithium acetate), and added to transformation buffer (a mixture of 240 μl 40% PEG 3350 and 36 μl 1 M lithium acetate). After incubation at 25°C for 30 min, 35 μl of DMSO was added, and the entire mixture was incubated at 30°C for 20 min, resuspended, and then plated on selective media.

Strain Construction

A list of strains generated or used in this study is provided (Table S3). A haploid strain expressing *S. castellii* Dcr1ΔC (comprising Tyr17–Glu356) from its native promoter was constructed by two-step homologous recombination in DPB277, as follows: An *S. cerevisiae URA3* expression cassette (amplified from pYES2.1, Invitrogen) was used to replace the open reading frame of *DCR1* by transformation and selection of transformants on SC–ura plates to generate DPB278; the *URA3* cassette was subsequently replaced by the open reading frame encoding Dcr1ΔC by transformation and selection on 5-FOA to generate DPB437. A control strain in which the full-length open reading frame of *DCR1* was used for replacement (DPB406) was generated similarly.

Expression Plasmid Construction

S. castellii DCR1 or *DCR1ΔC* was cloned into pYES2.1 (Invitrogen) to produce the galactose-inducible expression plasmids pYES2.1-ScDcr1 and pYES2.1-ScDcr1ΔC, respectively. Plasmids were transformed into DPB318, and expression was induced by growth in SC–ura containing 1% galactose and 1% raffinose.

Blots

Strains

Strains used in Figure 1E were DPB277, DPB278, DPB406, DPB437, DPB005, DPB318, DPB318 transformed with pYES2.1-Dcr1, and DPB318 transformed with pYES2.1-Dcr1ΔC; in Figure S1F were DPB005, DPB318, DPB318 transformed with pYES2.1-Dcr1, and DPB318 transformed with pYES2.1-Dcr1ΔN; and in Figure S5D were DPB005, DPB318, DPB318 transformed with pYES2.1-Dcr1, and DPB318 transformed with pAG416Gal-Dicer (Table S3 and Table S4).

RNA Blots

Total RNA was isolated using the hot-phenol method. Small-RNA blots were performed using 10–20 μg total RNA per lane and carbodiimide-mediated cross-linking to the membrane (Pall et al., 2007). Blots were hybridized with the following DNA probes radiolabeled at their 5′ termini: *S. castellii* siRNA sc1056, 5′-CTATCTTCATCGATTACCATCTA; *S. castellii* U6 small nuclear RNA, 5′-TATGCAGGGGAACTGCTGAT. To detect any siRNAs (including siRNA sc1056) deriving from the 5′ arm of the palindrome of substrate E (Figure 5E), the RNA blot in Figure S5D was hybridized with a body-labeled RNA probe corresponding to sequence from *S. castellii* sc1056:165468–165756(–), which was complementary to this arm.

Immunoblots

Three OD600 units of cells were resuspended in 100 ml H_2O. After adding 160 μl of extraction buffer (1.85 M NaOH, 7.4% β-mercaptoethanol), cells were incubated on ice for 10 min. 160 μl of 50% trichloroacetic acid was added, and cells were incubated on ice for an additional 10 min. Precipitated material was collected by centrifugation, and the supernatant was discarded. The tube was washed with 500 μl of 1 M Tris pH 8.0, centrifuged briefly, and the supernatant was discarded. The pellet was vigorously resuspended in 150 μl of 1X Laemlli sample buffer and boiled for 4 min. As a positive control, lysate from HEK293T cells was prepared by sonication in sonication buffer (20 mM Tris-HCl pH 8.0, 100 mM KCl, 0.2 mM EDTA) and combined with an equal volume of 2X Laemlli sample buffer. Samples (15 μl each) were resolved by SDS-PAGE, transferred to poly(vinylidene difluoride) in CAPS-ethanol pH 10, and probed sequentially with anti-Dicer (Abcam, ab14601) and anti-actin (Abcam, ab8224). Immunoblots were developed with HRP-conjugated anti-mouse antibody and enhanced chemiluminescence (Amersham).

Small-RNA Sequencing and Analysis

Sequencing Libraries

Standard single-turnover reactions were performed with the following modifications. 500 bp body-labeled dsRNA substrates contained 5′-monophosphate termini, and tRNA was omitted from dsRNA dilutions. For each enzyme, separate reactions were performed using dsRNA corresponding to fragments of the genes encoding *Renilla* luciferase and green fluorescent protein (GFP). Reactions were performed in a volume of 400 μl, with components at the same concentrations as in the standard reactions. Reactions were incubated at room temperature for 90 s and quenched by addition to an equal volume of phenol supplemented with 1/10 volume 3 M NaCl and 1/74 volume 0.5 M EDTA, pooling reactions performed with the same enzyme but different dsRNA substrates. Total RNA was isolated from dicing reactions by phenol extraction and precipitation. Small-RNA cDNA libraries were prepared as described (Grimson et al., 2008) and sequenced using the Illumina SBS platform.

Analysis

After removing the adaptor sequences, reads representing the small RNAs were collapsed to a non-redundant set, and 14–30 nt sequences were mapped to the appropriate template (i.e., *Renilla* luciferase or GFP), allowing no mismatches and recovering all hits (Table S1). To detect phasing, the frequencies of same-strand distances separating all 23 nt 5′-end pairs mapping to the substrate were calculated separately for each substrate as described (Drinnenberg et al., 2009). The frequencies of opposite-strand distances were calculated similarly, except that the 5′ ends of 23 nt reads mapping to the (–)-strand were first converted into the corresponding 5′ end on the (+)-strand that was generated by the same RNase III cleavage event (i.e., position *n* on the (–)-strand was mapped to position *n* + 3 on the (+)-strand). Each set of distance frequencies was then normalized to the total number of 5′-end pairs. Same-strand and opposite-strand relative frequencies were averaged between the GFP and *Renilla* luciferase substrates. The reported relative frequency of 5′-end pairs is the average of the same- and opposite-strand frequencies.

SUPPLEMENTAL REFERENCES

Abrahams, J.P., and Leslie, A.G. (1996). Methods used in the structure determination of bovine mitochondrial F1 ATPase. Acta Crystallogr. D Biol. Crystallogr. *52*, 30–42.

Adams, P.D., Grosse-Kunstleve, R.W., Hung, L.W., Ioerger, T.R., McCoy, A.J., Moriarty, N.W., Read, R.J., Sacchettini, J.C., Sauter, N.K., and Terwilliger, T.C. (2002). PHENIX: building new software for automated crystallographic structure determination. Acta Crystallogr. D Biol. Crystallogr. *58*, 1948–1954.

Brünger, A.T., Adams, P.D., Clore, G.M., DeLano, W.L., Gros, P., Grosse-Kunstleve, R.W., Jiang, J.S., Kuszewski, J., Nilges, M., Pannu, N.S., et al.. (1998). Crystallography & NMR system: A new software suite for macromolecular structure determination. Acta Crystallogr. D Biol. Crystallogr. *54*, 905–921.

Collaborative Computational Project, Number 4. (1994). The CCP4 suite: programs for protein crystallography. Acta Crystallogr. D Biol. Crystallogr. *50*, 760–763.

de La Fortelle, E., and Bricogne, G. (1997). Maximum-likelihood heavy-atom parameter refinement for multiple isomorphous replacement and multiwavelength anomalous diffraction methods. In Methods in Enzymology, C.W. Carter and R.M. Sweet, eds. (San Diego: Academic Press), pp. 472–494.

Emsley, P., and Cowtan, K. (2004). Coot: model-building tools for molecular graphics. Acta Crystallogr. D Biol. Crystallogr. *60*, 2126–2132.

Jones, T.A., Zou, J.Y., Cowan, S.W., and Kjeldgaard, M. (1991). Improved methods for building protein models in electron density maps and the location of errors in these models. Acta Crystallogr. A *47*, 110–119.

Liu, L., Botos, I., Wang, Y., Leonard, J.N., Shiloach, J., Segal, D.M., and Davies, D.R. (2008). Structural basis of toll-like receptor 3 signaling with double-stranded RNA. Science *320*, 379–381.

Macrae, I.J., Zhou, K., Li, F., Repic, A., Brooks, A.N., Cande, W.Z., Adams, P.D., and Doudna, J.A. (2006). Structural basis for double-stranded RNA processing by Dicer. Science *311*, 195–198.

Otwinowski, Z., and Minor, W. (1997). Processing of X-ray diffraction data collected in oscillation mode. In Methods in Enzymology, C.W. Carter and R.M. Sweet, eds. (San Diego: Academic Press), pp. 307–326.

Pall, G.S., Codony-Servat, C., Byrne, J., Ritchie, L., and Hamilton, A. (2007). Carbodiimide-mediated cross-linking of RNA to nylon membranes improves the detection of siRNA, miRNA and piRNA by Northern blot. Nucleic Acids Res. *35*, e60.

Scannell, D.R., Frank, A.C., Conant, G.C., Byrne, K.P., Woolfit, M., and Wolfe, K.H. (2007). Independent sorting-out of thousands of duplicated gene pairs in two yeast species descended from a whole-genome duplication. Proc. Natl. Acad. Sci. USA *104*, 8397–8402.

Suk, K., Choi, J., Suzuki, Y., Ozturk, S.B., Mellor, J.C., Wong, K.H., MacKay, J.L., Gregory, R.I., and Roth, F.P. (2011). Reconstitution of human RNA interference in budding yeast. Nucleic Acids Res. *39*, e43.

Vagin, A., and Teplyakov, A. (2000). An approach to multi-copy search in molecular replacement. Acta Crystallogr. D Biol. Crystallogr. *56*, 1622–1624.

Weeks, C.M., and Miller, R. (1999). The design and implementation of SnB version 2.0. J. Appl. Cryst. *32*, 120–124.

Wu, H., Henras, A., Chanfreau, G., and Feigon, J. (2004). Structural basis for recognition of the AGNN tetraloop RNA fold by the double-stranded RNA-binding domain of Rnt1p RNase III. Proc. Natl. Acad. Sci. USA *101*, 8307–8312.

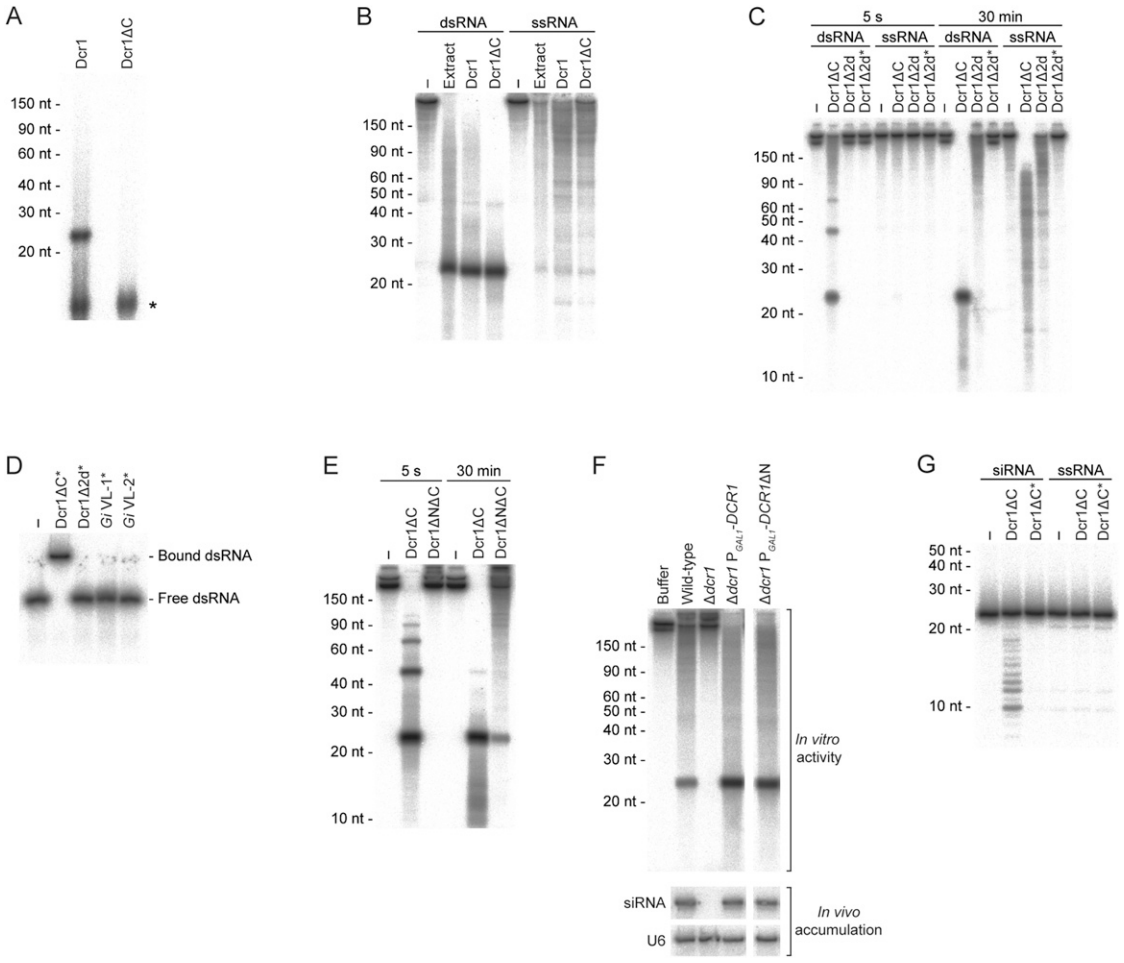

Figure S1. Characterization of Dcr1 Variants, Related to Figure 1

(A) Analysis of contaminating RNA in purified *K. polysporus* Dcr1 and Dcr1ΔC. Nucleic acid was isolated from the indicated purified protein by phenol extraction, RNA was 3′ end-labeled with cordycepin, and products were resolved by denaturing PAGE. A background band observed in cordycepin-mediated labeling reactions is indicated (*).

(B) Specificity of purified Dcr1 and Dcr1ΔC for dsRNA. Body-labeled 500 bp dsRNA or 500 nt ssRNA was incubated with buffer only (–), extracts prepared from wild-type *K. polysporus* (Extract), or the indicated purified protein under standard single-turnover conditions. Products were resolved by denaturing PAGE.

(C) Activity of *K. polysporus* Dcr1Δ2d, which spans Ser15 to Met260. Body-labeled 500 bp dsRNA or 500 nt ssRNA was incubated for the indicated time with buffer only (–) or the indicated purified protein (Dcr1Δ2d*, Dcr1Δ2d containing the E224Q active-site mutation) under standard single-turnover conditions. Products were resolved by denaturing PAGE.

(D) Binding of Dcr1ΔC and its variants. A trace amount of body-labeled 500 bp dsRNA was incubated with buffer only (–) or 3 nM of the indicated purified protein (Dcr1ΔC* and Dcr1Δ2d*, variants containing the E224Q active-site mutation; *Gi* VL-1* and *Gi* VL-2*, Dcr1ΔC variants with the E224Q active-site mutation and *Gi*Dicer loop-region substitutions) and separated by native gel electrophoresis.

(E) Activity of *K. polysporus* Dcr1ΔNΔC. Body-labeled 500 bp dsRNA present at 4.67 nM was incubated for the indicated time with buffer only (–) or 1 μM of the indicated purified protein. Products were resolved by denaturing PAGE.

(F) Comparison of in vitro activity with in vivo product accumulation in strains expressing the corresponding Dcr1 variants. Top: Body-labeled 500 bp dsRNA was incubated with extracts from *S. castellii* strains with the indicated deletions, additions, and replacements. Bottom: An RNA blot with samples from the same strains was probed for an endogenous siRNA, then reprobed for U6 small nuclear RNA.

(G) Processing of siRNA duplexes by *K. polysporus* Dcr1ΔC. A 23 nt siRNA duplex containing one 5′ end-labeled strand (siRNA) or a single-stranded end-labeled 23 nt RNA (ssRNA) was incubated with buffer only (–), wild-type Dcr1ΔC (WT), or an active-site mutant of Dcr1ΔC (Dcr1ΔC*) for 30 min. RNA and protein were present at 1 nM and 30 nM, respectively. Products were resolved by denaturing 20% PAGE.

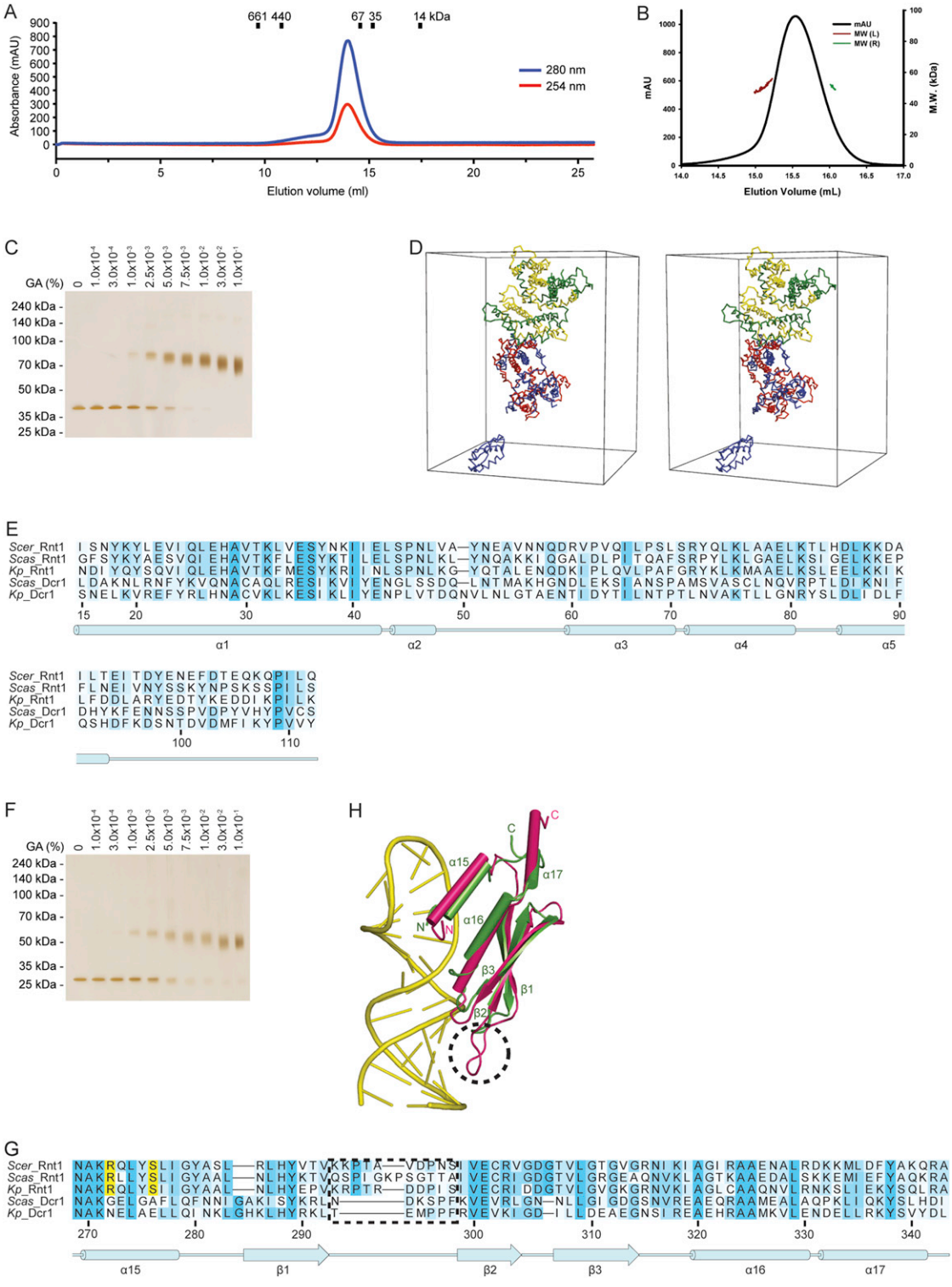

Figure S2. Analysis of Dcr1ΔC Sequence and Structure, Related to Figure 2

(A) Gel-filtration profile of Dcr1ΔC. Molecular weights of standards are shown above the absorbance trace. The expected molecular weights for the monomeric and dimeric forms of Dcr1ΔC are 39 kDa and 79 kDa, respectively.

(B) Multi-angle light scattering (MALS) analysis of Dcr1Δ2d. The unique fraction from gel filtration (black trace) had a molecular weight of 51 kDa (brown and green traces) over the peak. The expected molecular weights for the monomeric and dimeric forms of Dcr1Δ2d are 28 kDa and 57 kDa, respectively.

(C) Glutaraldehyde crosslinking of Dcr1ΔC. Dcr1ΔC was incubated with the indicated glutaraldehyde (GA) concentration, reactions were analyzed by SDS-PAGE, and proteins were visualized by silver staining. Also shown is the migration of protein standards with the indicated molecular weights. The faster migration of the crosslinked dimer species at high GA concentrations is attributable to the accumulation of intramolecular crosslinks.
(D) Stereo view of the contents of the asymmetric unit in the Dcr1ΔC crystal structure. We could trace four molecules composed of the NTD and RNase III domains (each shown in a different color), as well as one of the four dsRBD1 domains. Two of the remaining dsRBD1 domains were disordered, and the fourth exhibited very weak electron density.
(E) Sequence alignment of N-terminal domains found in RNase III enzymes from representative species in the *Saccharomyces* clade. Annotations of conservation, residue numbers, secondary structure, and species abbreviations are as in Figure 3A.
(F) Glutaraldehyde crosslinking of Dcr1ΔNΔC. Reactions using purified Dcr1ΔNΔC were performed and analyzed as in (C). The expected molecular weights for the monomeric and dimeric forms of Dcr1ΔNΔC are 29 kDa and 58 kDa, respectively.
(G) Sequence alignment of Dcr1 dsRBD1 and Rnt1 dsRBD, drawn as in (E). The preference of Rnt1 for AGNN tetraloops is conferred by residues in helix α1 of the dsRBD (Wu et al., 2004), which corresponds to helix α15 in Dcr1 (Figure 2B and Figure S2H). These residues, which are highlighted in yellow, are conserved among RNase III enzymes that recognize AGNN tetraloops but variant in Dcr1 enzymes. The β1-β2 loop that is especially short in the Dcr1 dsRBD1 is boxed.
(H) Superposition of the Dcr1ΔC dsRBD (green) on the Rnt1 dsRBD–hairpin complex (magenta and yellow, respectively; PDB: 1T4L). The β1-β2 loop of Rnt1 dsRBD is circled. The orientation of the Dcr1ΔC dsRBD is as in Figure 2B, central panel. Several residues at the N-terminus of the Dcr1ΔC dsRBD were deleted for clarity.

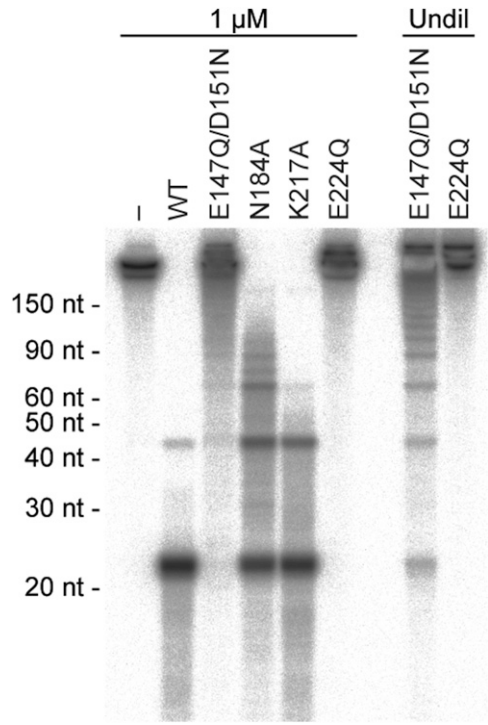

Figure S3. Activity of Dcr1ΔC Active-Site Mutants, Related to Figure 3

Body-labeled 500 bp dsRNA was incubated with buffer only (–), wild-type Dcr1ΔC (WT), or Dcr1ΔC variants with the indicated substitutions. Reactions contained dsRNA present at 140 pM and protein at the indicated final concentration, where undiluted (Undil) E147Q/D151N and E224Q mutants corresponded to 7.5 μM and 29.8 μM, respectively, without BSA. Products were resolved by denaturing PAGE.

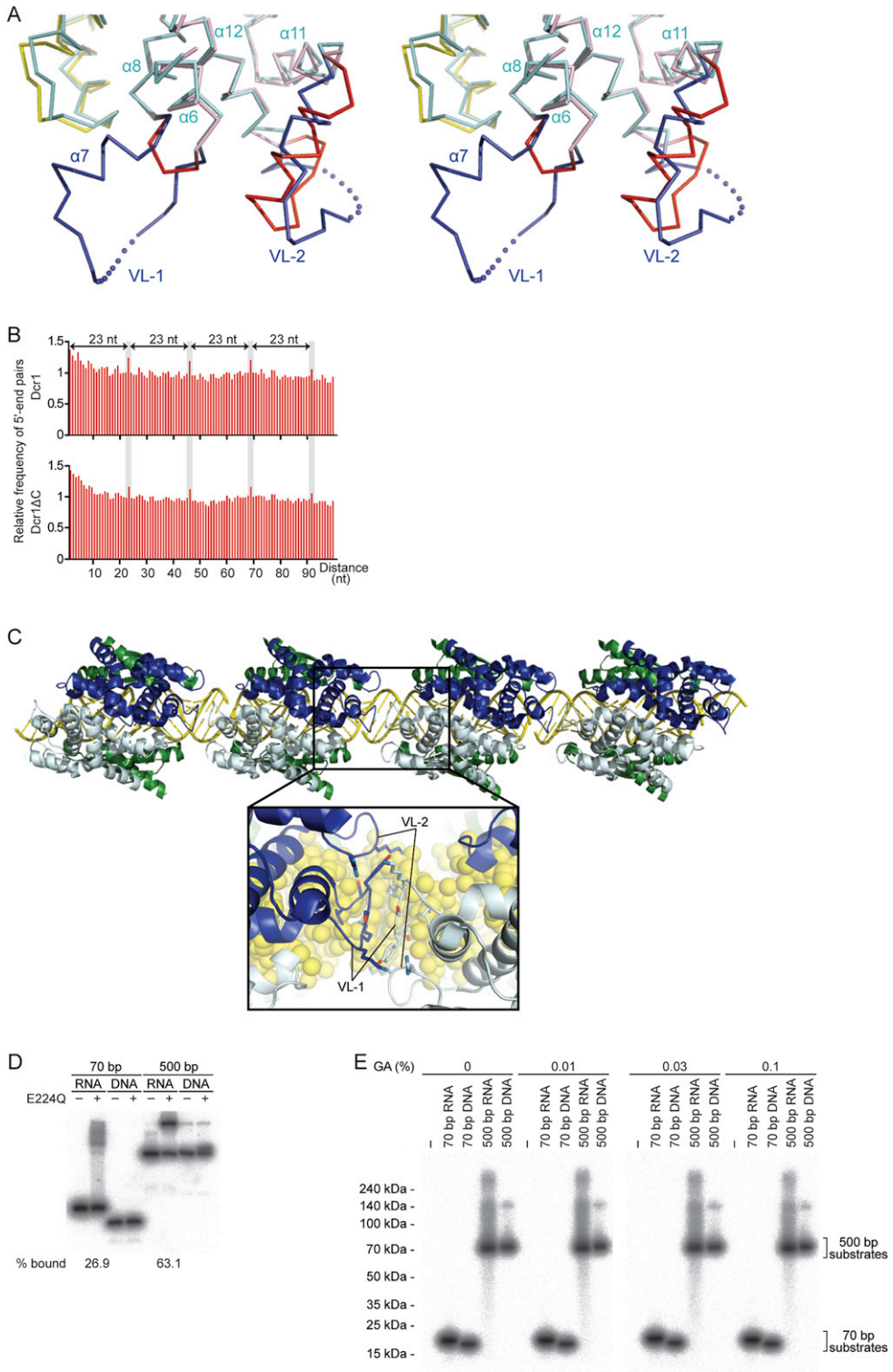

Figure S4. Binding and Cleavage within a dsRNA Duplex, Related to Figure 4

(A) Design of variable-loop substitutions in Dcr1ΔC. Stereo view of the superposition of the RNase III domain of Dcr1ΔC (cyan) with the RNase IIIa (yellow) and RNase IIIb (pink) domains of *Gi*Dicer. In our loop-swap experiments, either the VL-1 or VL-2 region of the RNase III domain of Dcr1ΔC (dark blue) was replaced with the corresponding region from the RNase IIIb domain of *Gi*Dicer (red). *Gi*Dicer was used for loop-swapping experiments because its structure is known and the RNase IIIb loops are expected to be solvent exposed based on structural modeling with a cognate dsRNA substrate (Macrae et al., 2006). Because the

mechanism of *Gi*Dicer does not involve intermolecular interactions between RNase III domains, the RNase IIIb loops are unlikely to contain amino acids that would mediate favorable intermolecular interactions. In contrast, the *Aa*RNase III loops can mediate crystal-packing interactions as shown in (C), suggesting that its variable loops might be able to mediate interdimer interactions in solution.

(B) Distribution of the intervals separating the 5′ termini of sequenced 23 nt products from in vitro dicing reactions using the indicated purified enzymes. Plotted is the relative frequency of each interval, when considering all pairs of reads less than 100 nt apart.

(C) Crystal-packing interactions between *Aa*RNase III dimers. The top view shows the crystal packing between adjacent complexes in the *A. aeolicus* RNase III enzyme (PDB code 2NUG). The bottom view shows a close up of the interface between adjacently positioned RNase III dimers. The color code is the same as in Figure 2A. The 22 nt dsRNA (yellow) forms a pseudo-continuous long dsRNA as a result of packing interactions in the crystal.

(D) Gel-shift analysis of binding reactions used for crosslinking in Figure 4F. BSA (–) or E224Q Dcr1ΔC (+) was incubated with the indicated nucleic acid, and reactions were subjected to native gel electrophoresis.

(E) Analysis of nucleic acid in crosslinking reactions. The RNA and DNA of Figure 4F were radiolabeled to allow their fate to be followed with a phosphorimager. This panel shows that crosslinking did not alter the migration of the RNA on SDS-PAGE and that a majority of the crosslinked bands did not overlap with RNA, even though gel-shift assays of the previous panel (D) indicated that a significant fraction of dsRNA was bound by Dicer. These results confirmed that the crosslinked species observed in Figure 4F represented protein-protein crosslinks.

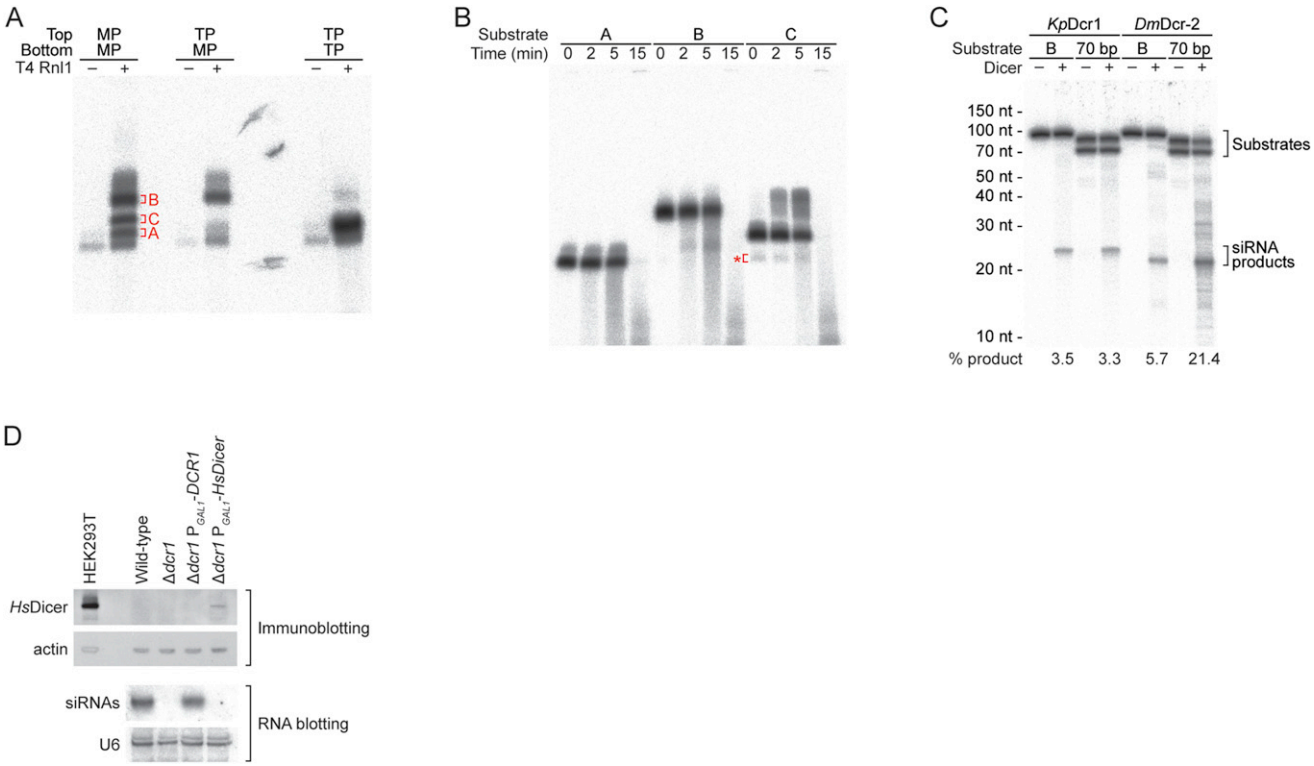

Figure S5. Generation, Confirmation, and Processing of Dicer Substrates, Related to Figure 5

(A) RNA ligation reactions that generated substrates A–C (Figure 5D). Annealed ssRNA duplexes containing the indicated 5′-ends (MP, monophosphate; TP, triphosphate) on the top and bottom strands were incubated without (–) or with (+) T4 RNA Ligase 1 (T4 Rnl1). Products were resolved by denaturing PAGE and distinguished as described in Extended Experimental Procedures.

(B) Limited hydrolysis of substrates A–C. Substrates were diluted in 1X Alkaline Hydrolysis Buffer (Ambion), heated at 90°C for the indicated time, and incubated on ice. Products were analyzed by denaturing PAGE (8% acrylamide, 90% formamide). Contaminating open duplex in the substrate C preparation is indicated (*).

(C) Comparison of Dicer activities on 70 bp substrates. Body-labeled substrates were incubated without (–) or with (+) *K. polysporus* Dcr1ΔC (*Kp*Dcr1) or *D. melanogaster* Dcr-2 (*Dm*Dcr-2) under multiple-turnover conditions (30 nM substrate and 10 nM protein). Substrate B, as in Figure 5D; 70 bp, a perfect duplex without T7-template–encoded ssRNA overhangs. Products were resolved by denaturing PAGE.

(D) Examination of human Dicer activity expressed in *S. castellii*. Top: Immunoblot probing for *H. sapiens* Dicer (*Hs*Dicer) in *S. castellii* strains with the indicated deletions and additions. Lysates prepared from HEK293T cells that endogenously express *Hs*Dicer served as a positive control. Bottom: RNA blot with samples from the same strains was probed for endogenous siRNAs derived from a palindromic RNA (corresponding to substrate E in Figure 5E), then reprobed for U6 small nuclear RNA. Although *Hs*Dicer protein was expressed in *S. castellii*, no siRNAs derived from the palindromic RNA were detected. These results suggest that human Dicer is not able to process the *S. castellii* substrate in vivo, which is consistent with the inability of a canonical Dicer to generate siRNAs from this palindromic RNA in vitro (Figure 5E). However, additional factors, such as expression level, localization, and interactions with other proteins, might have impaired the activity of human Dicer in this heterologous expression system.

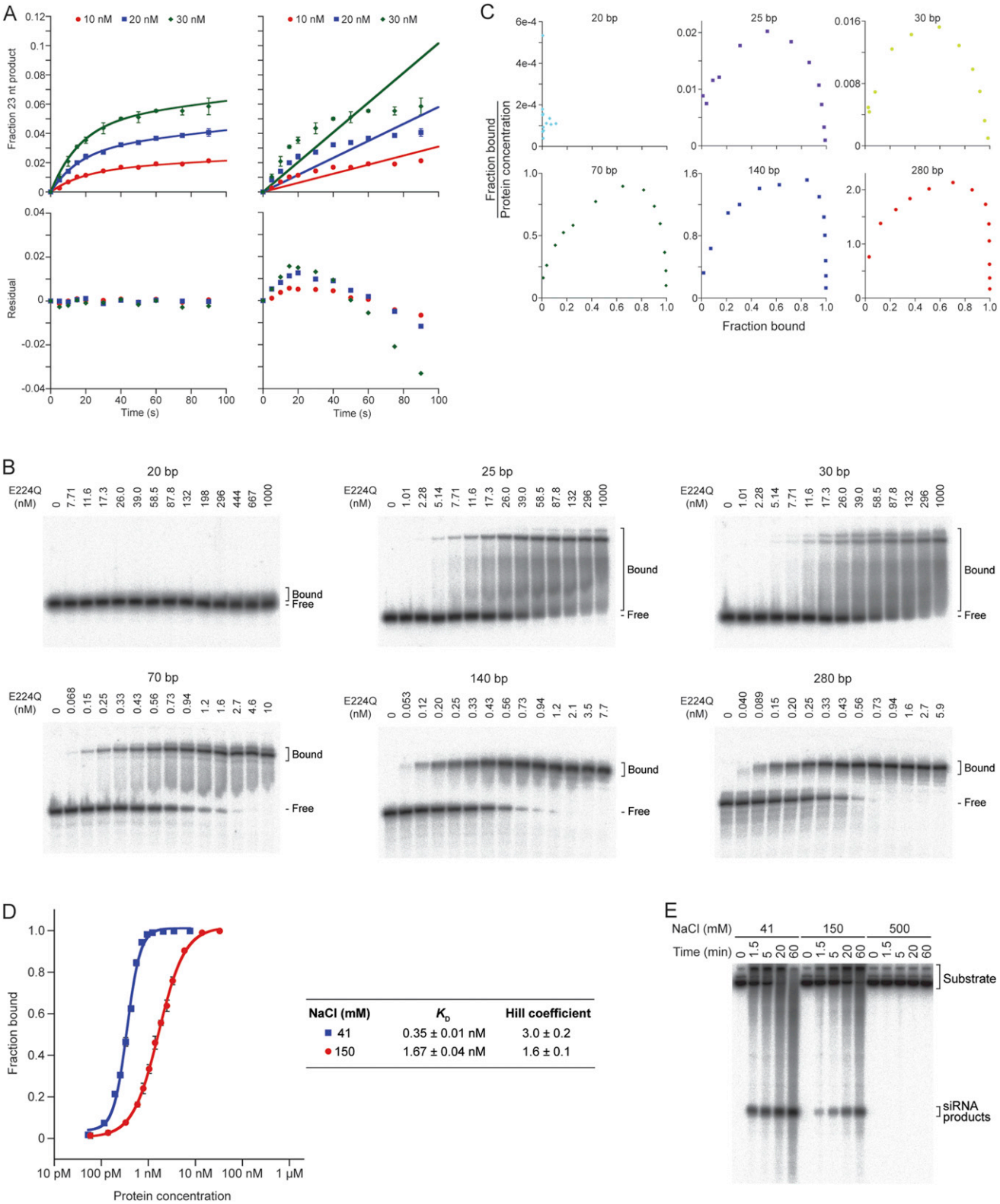

Figure S6. Analysis of Multiple-Turnover Kinetics and Cooperative Binding, Related to Figure 6

(A) Comparison of linear and biphasic fits to the data of Figure 6B. Data were fit to a double-exponential (left) or linear (right) function, and the resulting least-squares fit line (top) and residuals (bottom) were plotted. This analysis confirmed that the data are more appropriately described by a double-exponential function.

(B) Representative gel-shift assays. Trace amounts of body-labeled dsRNA of the indicated length were incubated with increasing amounts of protein and subjected to native gel electrophoresis.

(C) Scatchard plots of the binding data of Figure 6F. The concavity of the plots observed for substrates > 20 bp indicates positive cooperativity. In contrast to the full-length enzyme, Dcr1ΔC was less prone to aggregation and could be purified away from contaminating RNA (Figure S1A), which made it suitable for biochemical studies. Nonetheless, the observed cooperativity of Dcr1ΔC strongly implies that the full-length enzyme also binds cooperatively to dsRNA substrates, because although the deletions that convert full-length Dcr1 to Dcr1ΔC might decrease interdimer interactions and thereby decrease binding cooperativity, they would be unlikely to increase binding cooperativity.

(D) Binding isotherms for E224Q Dcr1ΔC binding to 140 bp dsRNA at low (41 mM) or physiological (150 mM) monovalent ion concentrations. Data points represent average values (n = 3; error bars indicate standard deviation). Solid lines show the best fit to the Hill equation, which produced the dissociation constants (K_D) and Hill coefficients shown to the right.

(E) Product accumulation under multiple-turnover conditions as a function of salt concentration. Body-labeled 500 bp dsRNA present at 14 nM (which corresponded to ~300 nM non-overlapping 23 bp sites) was incubated with 30 nM Dcr1ΔC for the indicated time with the indicated final concentration of NaCl.

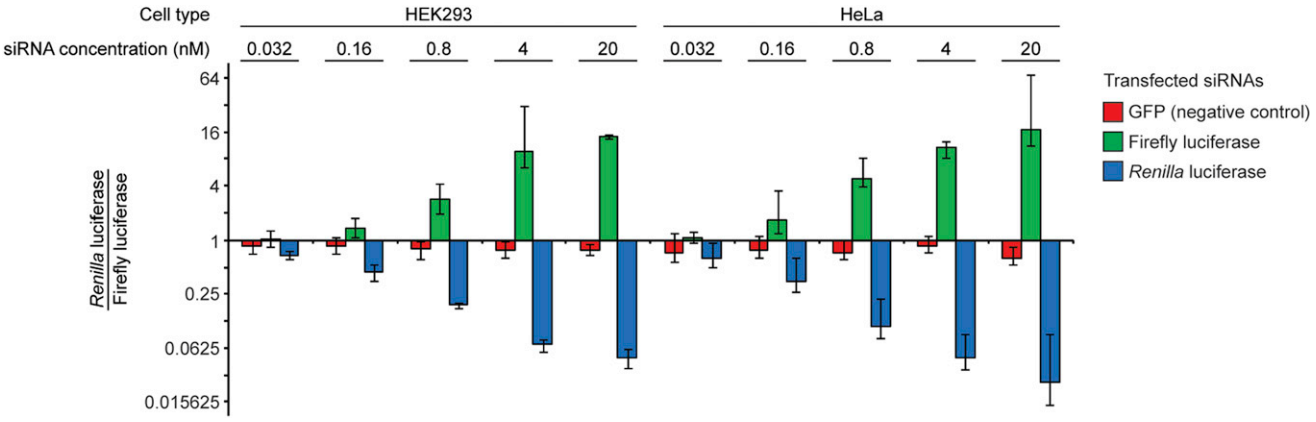

Figure S7. Using siRNAs Generated by Budding-Yeast Dicer for Mammalian Gene Knock-Down, Related to Figure 7

Shown is the ratio of *Renilla* luciferase to firefly luciferase following transfection of the indicated cell type with the indicated siRNAs. Plotted are the geometric means, normalized to the geometric means for cells in which no siRNAs were transfected. Error bars represent the largest and the smallest values among 6 replicates (from two independent experiments).

siRNA preparation. Separate reactions were performed using dsRNA corresponding to fragments of the genes encoding *Renilla* luciferase, firefly luciferase, and green fluorescent protein (GFP). Reactions were performed in a volume of 1 ml with 339 nM Dcr1(1–384) and 10 ng/μl dsRNA. Reactions were incubated at room temperature for 45 min and quenched by addition of 1/5 volume 50 mM EDTA supplemented with 1.5 M NaCl. After addition of 1 ml dsRNA Storage Buffer, total RNA was isolated by phenol extraction and precipitation, and siRNAs were enriched for using RNA Purification Column 2 (Genlantis). To confirm the production of siRNA duplexes, a portion of the preparation was analyzed by native 15% PAGE.

Cell culture and luciferase assays. One day prior to transfection, HeLa or HEK293 cells were seeded into 24-well plates at a density of 0.5–1 × 10^5 cells/well in 500 μl of DMEM supplemented with 10% FBS. Cells were transfected in triplicate with 100 ng each of pIS0 and pIS1 (expressing firefly and *Renilla* luciferase genes, respectively) and 5-fold serial dilutions (20 nM to 32 pM) of siRNA products. Twenty-two hours later, cells were washed with PBS, and *Renilla* and firefly luciferase levels were determined using the Dual-Luciferase Reporter Assay System (Promega) according to the manufacturer's directions.

Table S1. Analysis of Small-RNA Libraries, Related to Figure 1

	K. polysporus Dcr1		*K. polysporus* Dcr1ΔC	
All substrate-matching reads	290550	(100)	839110	(100)
23 nt substrate-matching reads	232873	(80.1)	588945	(70.2)
GFP				
All reads	102732	(35.4)	314579	(37.5)
23 nt reads	74065	(25.5)	202214	(24.1)
Luciferase				
All reads	187818	(64.6)	524531	(62.5)
23 nt reads	158808	(54.7)	386731	(46.1)

Numbers in parentheses indicate the percent of reads compared to total number of substrate-matching reads.

Table S2. Crystallographic Data Statistics for *K. polysporus* Dcr1ΔC and Dcr1Δ2d, Related to Figure 2

Structure	Dcr1ΔC		Dcr1Δ2d
Crystal	Native	SeMet	Native
Data collection			
Space group	$P2_12_12_1$	$P2_12_12_1$	$P2_12_12_1$
Cell dimensions (*a*, *b*, *c* [Å])	101.0, 113.0, 135.7	101.0, 113.0, 134.7	58.9, 96.4, 101.4
Wavelength (Å)	0.9795	0.9792	0.9792
Resolution (Å)[a]	50.00–2.30 (2.38–2.30)	50.00–3.50 (3.56–3.50)	50.00–1.97 (2.04–1.97)
R_{sym} [a]	0.095 (0.636)	0.157 (0.540)	0.094 (0.458)
$I/\sigma(I)$ [a]	27.3 (2.8)	25.5 (9.8)	16.7 (2.1)
Completeness (%)[a]	99.7 (97.7)	100.0 (100.0)	97.9 (96.1)
Unique reflections[a]	69,722 (6718)	38,291 (1758)	40,348 (406)
Redundancy[a]	10.0 (8.8)	7.7 (7.8)	5.6 (4.1)
Structural Refinement			
Resolution (Å)	43.41–2.29		48.21–1.97
Number of reflections	64,882		40,311
R_{work}/R_{free}	17.51/21.91 (20.72/27.63)		19.30/23.75 (34.95/39.57)
Number of Atoms			
Protein	8157		3699
Ion	4		-
Water	467		262
Average B-factors (Å^2)			
Protein	46.21		26.04
Ion	48.03		-
Water	41.18		30.47
Rmsd Values			
Bond lengths (Å)	0.010		0.007
Bond angles (º)	0.974		0.947

[a] Values for the highest resolution shell are in parentheses.

Table S3. Yeast Strains Used and Generated in This Study, Related to the Experimental Procedures

Strain	Genotype	Species	Reference
KpolWT	Wild-type	*K. polysporus* DSM70294	(Scannell et al., 2007)
DPB277	*MATα hoΔ ura3::EGFP(S65T)-KanMX6 Flag$_3$-AGO1*	*S. castellii* CBS4310	This study
DPB278	*MATα hoΔ ura3::EGFP(S65T)-KanMX6 Flag$_3$-AGO1 dcr1::ScerURA3*	*S. castellii* CBS4310	This study
DPB406	*MATα hoΔ ura3::EGFP(S65T)-KanMX6 Flag$_3$-AGO1 dcr1::DCR1*	*S. castellii* CBS4310	This study
DPB437	*MATα hoΔ ura3::EGFP(S65T)-KanMX6 Flag$_3$-AGO1 dcr1::DCR1ΔC*	*S. castellii* CBS4310	This study
DPB005	*MATα hoΔ ura3-1*	*S. castellii* CBS4310	(Drinnenberg et al., 2009)
DPB318	*MATα hoΔ ura3-1 dcr1Δ*	*S. castellii* CBS4310	(Drinnenberg et al., 2009)

Table S4. Plasmids Generated in This Study, Related to the Experimental Procedures

Plasmid	Description
pRSF-KpDcr1	*E. coli* expression plasmid, *K. polysporus DCR1*
pRSF-KpDcr1ΔC	*E. coli* expression plasmid, *K. polysporus DCR1*(15–355)
pRSF-KpDcr1ΔC(E147Q/D151N)	*E. coli* expression plasmid, *K. polysporus DCR1*(15–355) with E147Q/D151N
pRSF-KpDcr1ΔC(N184A)	*E. coli* expression plasmid, *K. polysporus DCR1*(15–355) with N184A
pRSF-KpDcr1ΔC(K217A)	*E. coli* expression plasmid, *K. polysporus DCR1*(15–355) with K217A
pRSF-KpDcr1ΔC(E224Q)	*E. coli* expression plasmid, *K. polysporus DCR1*(15–355) with E224Q
pRSF-KpDcr1Δ2d	*E. coli* expression plasmid, *K. polysporus DCR1*(15–260)
pRSF-KpDcr1Δ2d(E224Q)	*E. coli* expression plasmid, *K. polysporus DCR1*(15–260) with E224Q
pRSF-KpDcr1ΔNΔC	*E. coli* expression plasmid, *K. polysporus DCR1*(107–355)
pRSF-KpDcr1(1–384)	*E. coli* expression plasmid, *K. polysporus DCR1*(1–384)
pRSF-KpDcr1ΔC(*Gi* VL-1)	*E. coli* expression plasmid, *K. polysporus DCR1*(15–355) with H123–N143 replaced by P642–Y645 of *Gi*Dicer
pRSF-KpDcr1ΔC(E224Q, *Gi* VL-1)	*E. coli* expression plasmid, *K. polysporus DCR1*(15–355) with E224Q and with H123–N143 replaced by P642–Y645 of *Gi*Dicer
pRSF-KpDcr1ΔC(*Gi* VL-2)	*E. coli* expression plasmid, *K. polysporus DCR1*(15–355) with N195–M215 replaced by P697–D714 of *Gi*Dicer
pRSF-KpDcr1ΔC(E224Q, *Gi* VL-2)	*E. coli* expression plasmid, *K. polysporus DCR1*(15–355) with E224Q and with N195–M215 replaced by P697–D714 of *Gi*Dicer
pYES2.1-ScDcr1	2-micron plasmid, *S. castellii DCR1* under *GAL1* promoter
pYES2.1-ScDcr1ΔC	2-micron plasmid, *S. castellii DCR1*(17–356) under *GAL1* promoter
pYES2.1-ScDcr1ΔN	2-micron plasmid, *S. castellii DCR1*(111–610) under *GAL1* promoter
pAG416Gal-Dicer	*CEN* plasmid, *H. sapiens DICER* under *GAL1* promoter (Suk et al., 2011)